Stability and reactivity of metal nanoclusters supported on transition metal carbides

Hector Prats and Michail Stamatakis

Department of Chemical Engineering, University College London, Roberts Building, Torrington Place, London WC1E 7JE, UK

Corresponding author: Hector Prats (h.garcia@ucl.ac.uk)

Table S1. List of TM_n@TMCs for which the most stable configuration is 3D (i.e., tetrahedral), and relative stability to the most stable 2D configuration (i.e., square).

Cluster	Most stable 2D configuration (Figure S2)	Stability of the 2D configuration compared to the 3D one (eV)
Au_n@TiC	tC-M	0.29
Au_n@ZrC	tC-M	0.06
Au_n@HfC	tC-M	0.18
Au_n@cMoC	br-C	0.23
Pt_n@cMoC	tC-M	0.23
Au_n@cWC	br-C	0.31
Cu_n@cWC	br-C	0.14
Pt_n@cWC	tC-M	0.64

Table S2. Experimental and calculated lattice parameters for the bulk TMCs.

Structure	Materials Project ID	Lattice parameters (a, b, c) / Å*		Deviation / %
		Experimental	Calculated (PBE-D3)	
TiC	mp-631	4.328[1]	4.308	-0.46
ZrC	mp-2795	4.698[2]	4.694	-0.08
HfC	mp-21075	4.631[1]	4.624	-0.16
VC	mp-1282	4.165[1]	4.138	-0.65
NbC	mp-910	4.469[3]	4.460	-0.21
TaC	mp-1086	4.453[1]	4.456	0.07
hMoC	mp-2305	2.898, 2.898, 2.809[4]	2.904, 2.904, 2.819	0.22, 0.22, 0.34
cMoC	mp-2746	4.278[5]	4.348	1.63
hWC	mp-1894	2.91, 2.91, 2.84[6]	2.913, 2.913, 2.846	0.11, 0.11, 0.20
cWC	mp-13136	4.374[7]	4.366	-0.19

* If a = b = c only one value is indicated

Table S3. Surface C-vacancy formation energies for the cubic TMC slabs, computed as $E_{f,C-vac} = E_{TMC-vac} + E_C - E_{TMC}$ where $E_{TMC-vac}$ and E_{TMC} are the total DFT energies for the TMC slab with one surface C vacancy and the stoichiometric slab, respectively, and E_C is the atomic energy of a C atom in the most stable bulk phase (i.e., graphite).

TMC	$E_{f,C-vac}$ (eV)
TiC(001)	0.73
ZrC(001)	0.74
HfC(001)	1.07
VC(001)	-0.27
NbC(001)	-0.10
TaC(001)	0.23
c-MoC(001)	-1.91
c-WC(001)	-1.02

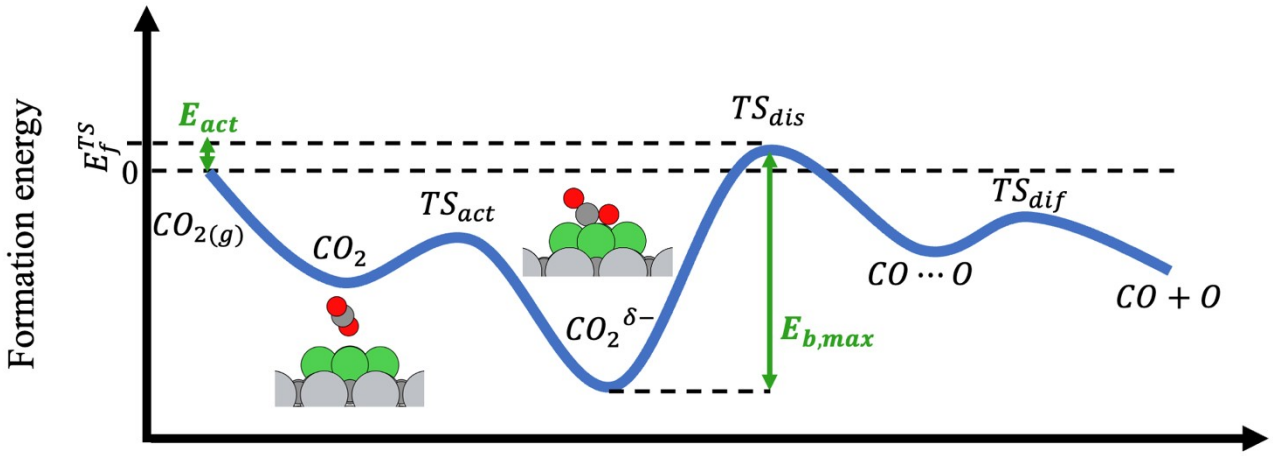

Figure S1. Example of the reaction profile of CO_2 adsorption and dissociation on a supported cluster with a very low activation energy (E_{act}) but a high energy barrier for dissociation ($E_{b,dis}$). Light grey and green spheres represent the metal atoms from the carbide and the supported cluster, respectively, and dark grey and red spheres represent carbon atoms and oxygen atoms, respectively.

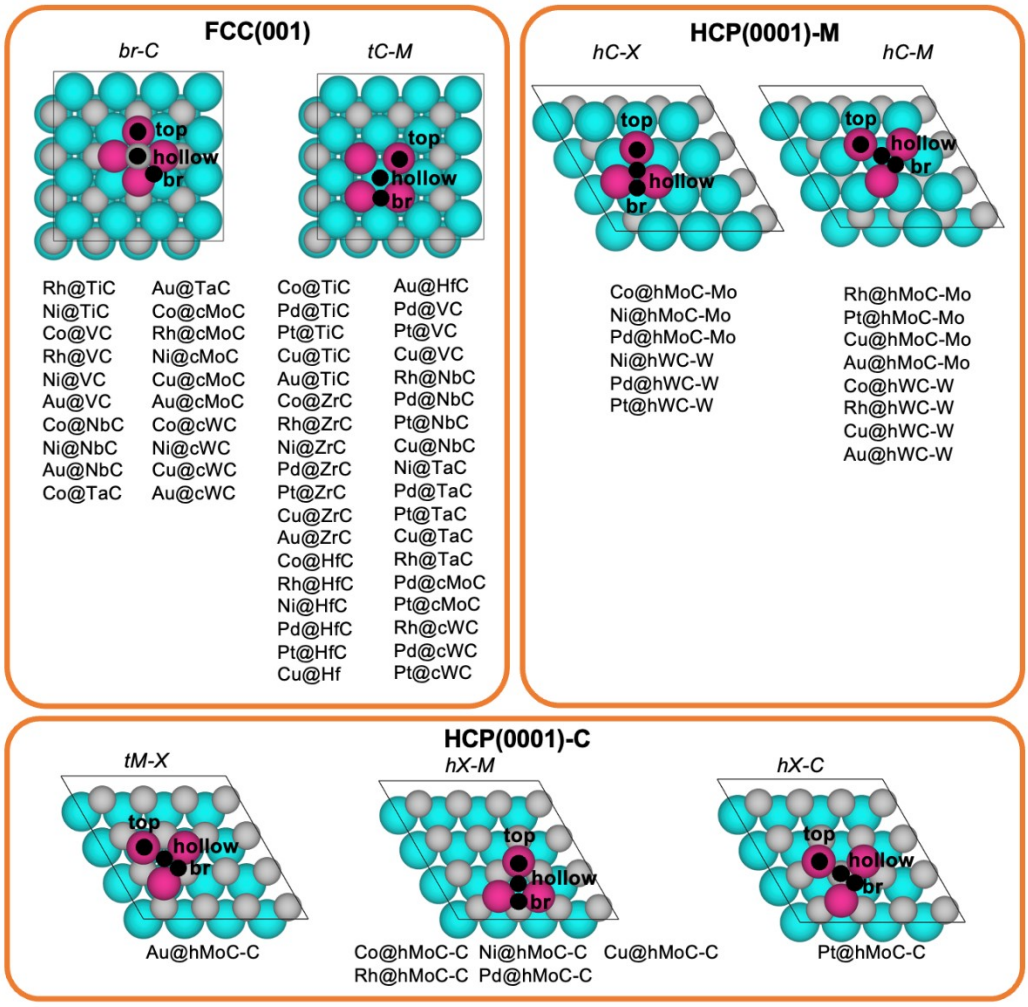

Figure S2. Geometry of all systems screened in this study and the corresponding adsorption sites considered for adsorption of species. The cluster configuration is shown in italics, following the notation from our previous work[8].

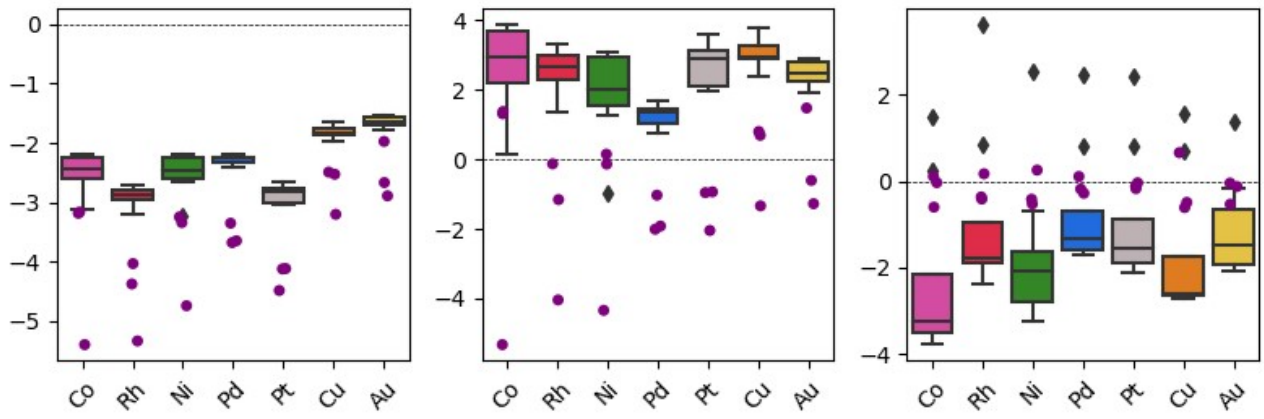

Figure S3. Box plots showing the distribution of E_{ads}, E_{agg} and E_{frag} grouped by metals for all 4-atom metal clusters supported on cubic TMCs. The values corresponding to the 3-atom clusters supported on hexagonal TMCs are plotted as purple dots.

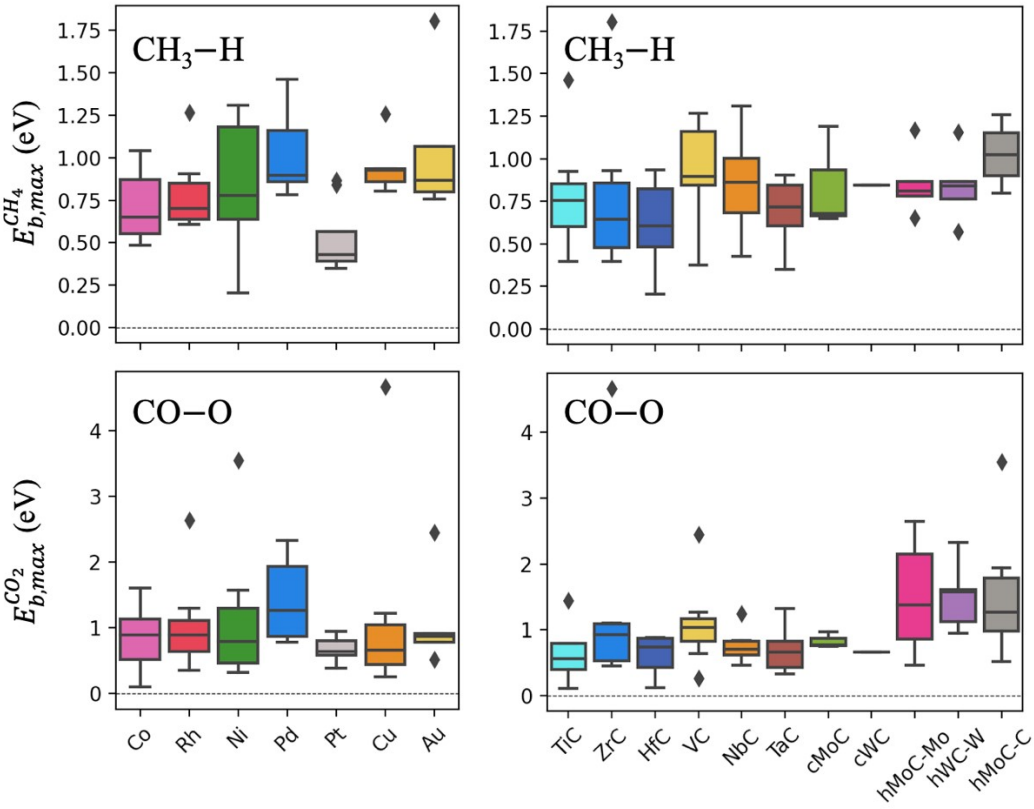

Figure S4. Distribution of $E_{b,max}$ for CH_4 (top) and CO_2 (bottom) dissociation for each metal (left) and TMC support (right).

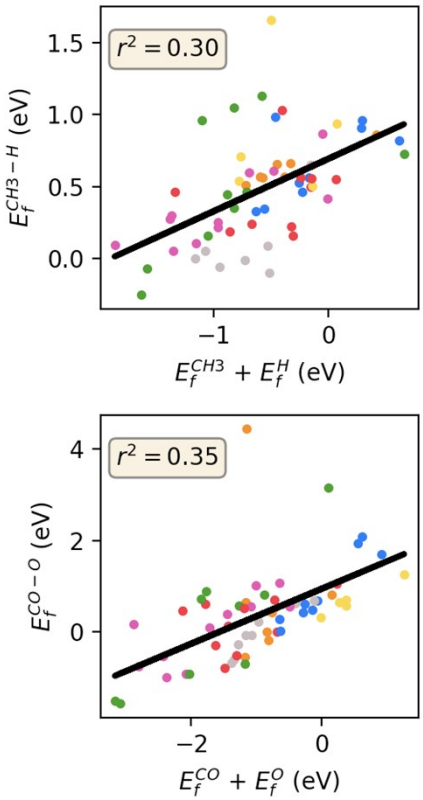

Figure S5. BEP relationship for CH_3 − H (top) and CO − O (bottom) bond dissociation on TM_n@TMCs. The points are coloured by cluster metal, following the colouring scheme used in all other plots. The equations of the regression lines are $y = 0.37x + 0.69$ (top) and $y = 0.60x + 0.94$ (bottom).

References

[1] K. Nakamura and M. Yashima, *Mater. Sci. Eng., B* 2008, **148**, 69-72

[2] A. N. Christensen, *Acta Chem. Scand.* 1990, **44**, 851-852

[3] G. Will and R. Platzbecker, *Zeitschrift für Anorg. un Allg. Chemie.* 2001, **627**, 2207

[4] A. Chrysanthou and P. Greivson, *J. Mater. Sci. Lett.* 1991, **10**, 145-146

[5] A. Fernández-Guillermet, J. Häglund and G. Grimvall, *Phys. Rev. B: Condens. Matter Mater. Phys.* 1992, **45**, 11557-11567

[6] L. E. Toth, Transition Metal Carbides and Nitrides, Academic Press, New York, 1971

[7] J. Yang and F. Gao, *Phys. B* 2012, **407**, 3527-3534

[8] H. Prats and M. Stamatakis, *J. Mater. Chem. A*. 2022, **10**, 1522-1534